Growth of Crystalline Tungsten Carbides Using 1,1,3,3- Tetramethyl-1,3-disilacyclobutane on a Heated Tungsten Filament

ARTICLE *in* THE JOURNAL OF PHYSICAL CHEMISTRY C · JANUARY 2013

Impact Factor: 4.77 · DOI: 10.1021/jp3112777

THE JOURNAL OF PHYSICAL CHEMISTRY C

Article

Growth of Crystalline Tungsten Carbides Using 1,1,3,3-Tetramethyl-1,3-disilacyclobutane on a Heated Tungsten Filament

Yujun Shi, Ismail Badran, Alexander Tkalych, Wang Hay Kan, and Venkataraman Thangadurai

J. Phys. Chem. C, **Just Accepted Manuscript** • DOI: 10.1021/jp3112777 • Publication Date (Web): 29 Jan 2013

Growth of Crystalline Tungsten Carbides Using 1,1,3,3-Tetramethyl-1,3-disilacyclobutane on a Heated Tungsten Filament

Yujun Shi*, Ismail Badran, Alexander Tkalych, Wang Hay Kan, Venkataraman Thangadurai

Department of Chemistry, University of Calgary, Calgary, Alberta, T2N 1N4

* Corresponding author: shiy@ucalgary.ca; Tel: 1-403-2108674; Fax: 1-403-2899488

Abstract

A method of forming crystalline tungsten carbides was reported by exposing the heated tungsten filament to 1,1,3,3- tetramethyl-1,3-disilacyclobutane (TMDSCB) in a hot-wire chemical vapor deposition process. Methyl radicals produced from the decomposition of TMDSCB on the filament serve as the carbon source. The formation of tungsten carbides was investigated by X-ray diffraction, cross-sectional scanning electron microscopy, and in-situ filament resistance measurements. A pure W_2C phase was formed at a high temperature of 2400 ºC after 1 - 2 hour exposure time with a growth rate of 4.4 $\mu m \cdot min^{-1}$. The growth of the W_2C layer is found to be a diffusion-controlled process. Our study at longer deposition time of 3 - 4 hours shows that once the metal filament is fully carburized to form W_2C, the carbon-rich WC phase starts to form on the outside layer upon further exposure to TMDSCB. A WC layer with no contamination from the W_2C phase was found to be formed at 2400 ºC and 4-hour deposition time.

Keywords

tungsten carbide, chemical vapor deposition, crystalline thin film, metal alloy, 1,1,3,3-tetramethyl-1,3-disilacyclobutane

Introduction

Metal filaments are essential in the hot wire chemical vapor deposition (HWCVD) process which has found wide applications in the deposition of silicon-containing thin films, diamond coatings, and polymer coatings.[1] In HWCVD, the metal filament, usually made of tungsten or tantalum, catalytically decomposes the source gas to form various reactive species which initiates the gas-phase reaction chemistry. It therefore, plays an important role in controlling the final mix of film growth precursors, and consequently, the film properties. On the other hand, the reactive species formed on the filaments also react with the metal itself, leading to the formation of metal alloys. Formation of metal silicides[2-6] and metal carbides[7-10] has been reported in the literature. Filament alloying changes its catalytic ability, causes the filament to age, and also affects the deposited film properties.[2,3,9,11] The effect is, in general, negative, and therefore should be avoided. However, Rye[7] showed that the evaporation of carbon from the carburized tungsten filament led to the growth of pure glassy carbon films. When investigating the role of the tungsten filament in the growth of polycrystalline diamond films, Moustakas[12] found that the filament was converted to α-W_2C, and the carburized form was more efficient in forming the diamond thin films.

Among the metal alloys formed in the hot filament used in HWCVD, tungsten carbides possess many unique mechanical, electronic and chemical properties that have led to their applications as anti-wear and corrosion-resistant coatings as well as thin-film diffusion barriers.[13,14] Since the discovery in 1973 by Levy and Boudart[15] that tungsten monocarbide (WC) show platinum-like behavior in the formation of water from H_2 and O_2, and the isomerization of 2,2-dimethylpropane to 2-methylbutane, a lot of efforts have been made in exploring tungsten carbides as heterogeneous catalysts for other reactions including the oxidation

of methanol[16, 17], H_2 evolution from water electrolysis[17], and ethylene hydrogenation.[18] Different types of tungsten carbide materials in the form of single crystal, carbide-modified single crystal, and polycrystalline thin films have been synthesized and their reactivity with various molecules have been studied.[19] Preparation of polycrystalline tungsten carbide thin films using plasma reactive deposition[20], and pulsed laser deposition[21] has been previously reported in the literatures. However, single-phase films of either WC or W_2C cannot be obtained from these methods. The formed products are usually a mixture of both phases. Deposition using magnetron sputtering[22-24] provides mixed results. Palmquist *et al.*[22] showed that a pure W_2C phase could be formed but WC could only be deposited as a minority phase. However, formation of both single-phase W_2C and WC films has been demonstrated using magnetron sputtering by tuning the deposition conditions.[17,23] Recently Beadle *et al.*[25] reported the formation of a phase-rich WC film with negligible W_2C component using thermal CVD with a gaseous mixture of C_3H_8, H_2 and Ar. Reports have also been found on preparing phase-pure WC film by carburizing a pre-cleaned W foil.[26,27] The carburization was performed by decomposing ethylene using a hot-filament sputter gun at 0.5 kV bias potential, followed by annealing the surface to 1200 K.

In this work, we report a method of forming polycrystalline film of tungsten carbides by exposing a heated tungsten filament to 1,1,3,3-tetramethyl-1,3-disilacyclobutane (TMDSCB) in a hot-wire CVD process. TMDSCB is a four-membered-ring compound which possesses a significant ring-strain energy.[28] Asides from TMDSCB, our group has also studied two other precursor gases, *i.e.*, 1-silacyclobutane (SCB)[5] and silane[6], in making tungsten alloys. It has been shown that exposure of W filaments to silane and SCB leads to the formation of tungsten silicides, whereas exposure to TMDSCB forms tungsten carbide. The difference in the nature of the tungsten alloys formed using various precursor molecules has been found to originate from

the different radical intermediates produced from the decomposition of precursor gas on the hot filament.[29,30,31] For TMDSCB, our previous study has shown that the dominant decomposition channel on a hot W filament is the formation of methyl radical according to equation (1).[29] The methyl radicals serve as the carbon source produced in-situ to carburize the filament, leading to the formation of tungsten carbides.[10]

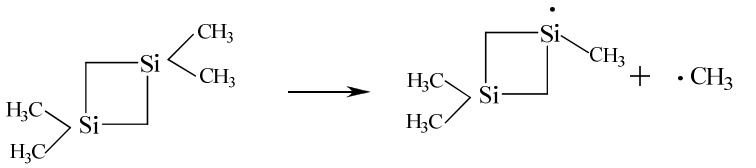

(1)

At temperatures lower than 2000 ºC with a fixed deposition time of 1 hour, it was found that both WC and W_2C were formed on the filament surface and the filament was partially carburized to from a W_2C layer toward the metal core.[10] However, whether the carbides are crystallined or not is not clear. To examine the effect of temperature and time on the formation of tungsten carbides and to understand the phases of tungsten carbide films on the heated W filaments for the possibility of forming a pure WC or W_2C layer, we recently performed a study in the temperature range of 2000 to 2400 ºC with the deposition time varied from 1 to 4 hours. The crystallinity of tungsten carbides was examined using X-ray diffraction (XRD). In addition, scanning electron microscopy (SEM) and in-situ filament resistance measurements were employed to monitor the growth of different phases of tungsten carbides on the W wires exposed to TMDSCB.

Experimental Details

Details of the HWCVD reactor to prepare tungsten carbides have been described previously.[31-34] A straight W filament (99.9%, Aldrich; D = 0.5 mm, L = 10 cm) was placed in a cylindrical stainless steel chamber (volume 7.1 L) and it was resistively heated by a DC power

supply (Aglient, N5744A). The temperature of the filament was measured by a two-color IR pyrometer (Chino Works). Prior to deposition, each new W filament was annealed by heating at 2000 ºC in 12 Torr of 1% H_2 in He gaseous mixture for 2 hours. This also serves to clean the reactor chamber wall from any deposits from previous runs. For each deposition, 12 Torr of the TMDSCB/He samples were introduced into the reactor via needle valves. Typical flow rate is 1 sccm. The pressure in the reactor was monitored by a capacitance manometer (MKS, type 626A). The concentration of the TMDSCB/He mixture used is 4%, which gave a partial pressure of TMDSCB at 0.48 Torr in the reactor. The gaseous mixture was prepared by entraining the room-temperature TMDSCB vapor in helium (99.995%, Praxair) after the liquid TMDSCB (97%, Starfire Systems) sample was degassed using three freeze-pump-thaw cycles. Formation of tungsten carbides was performed at filament temperatures ranging from 2000 to 2400 ºC and the deposition time from 1 to 4 hours. For each run, the filament temperature was kept constant by adjusting the supplied power. The current and voltage to the filament were monitored in situ with a LabVIEW program from which the power and resistance data can be obtained. After deposition, the metal filaments were cooled to room-temperature in the reactor and they were stored under vacuum after removal from the reactor. The film thickness was measured from the cross-sectional SEM images obtained from a field emission SEM (Philips XL30), operating at 20.0 kV.

The crystalline phases of the samples were characterized ex-situ using XRD. The XRD analysis was performed using a Bruker D8 Advance X-ray diffractometer with a Cu K_α radiation source (λ = 1.54 Å) operated at 40 kV and 40 mA. Samples were scanned in the 2θ range of 10 to 80°. Data was collected in a continuous mode with a step size of 9 second/step. The metal filaments were placed on the glass slides to record the XRD patterns. The room temperature

datasets were refined by conventional Rietveld method using the GSAS package with the EXPGUI interface.[35] A LeBail-like approach was used for the samples with highly preferred orientations, where background, scale factor, zero-point position, cell parameters, preferred orientations and profile coefficients for Pseudo-Voight / FCJ Asymmetric peak shape function were refined until the convergence was achieved. The average size of the crystallite particles was evaluated using the Scherrer formula.

$$s = \frac{K\lambda}{B\cos\theta} \qquad (2)$$

where λ is 0.154 nm from the Cu K_α radiation source, K is the shape factor which is taken as 0.9, B is the peak broadening represented by full width at half maximum in radian corrected for instrument broadening, and θ is the Bragg angle. The crystallite size was determined from the most intense peak in each phase.

Results and Discussions

Figures 1a and 1b showed the XRD patterns obtained for the alloyed metal filaments after each deposition run at different temperatures for a fixed time of 1 hour and 2 hours, respectively. All spectra shown were obtained after the broad background signals from the amorphous glass slides were removed. The XRD characterization of a new W filament showed three main peaks at 2θ = 40.6, 58.6, and 73.5º with an intensity ratio of 1.0 : 2.1 : 2.8. This is representative of the body-centered cubic tungsten (JCPDS no. 00-001-1203).[36] After exposing the W filaments to the gaseous mixture of TMDSCB and He at high temperatures of 2000 to 2400 ºC, peaks characteristic of crystalline phases of WC and W_2C started to come out. In the 2θ range of 10 to 80º, the diffraction peaks due to W_2C were observed at 38.2º (002), 39.8º (101), 52.5º (102), 62.2º (110), 70.0º (103), and 75.2º (112) (JCPDS no. 03-065-3896).[37] The peaks at 31.7º (001),

35.8º (100), 48.5º (101), 64.2º (110), 73.2º (111), 75.6º (200), and 77.3º (102) were from hexagonal WC (JCPDS no. 03-065-4539).[38] The labels in the brackets are the respective diffraction planes. Rietveld refinement on the powder XRD (PXRD) further confirmed that the cell parameters of W_2C phase (space group of P-31m (162) with average value of a = 5.19(2) Å, c = 4.73(1) Å and V = 110(1) Å^3) and WC phase (space group of P-6m2 (187) with average value of a = 2.909(7) Å, c = 2.841(3) Å and V = 20.8(1) Å^3) are in very good agreement with the results reported previously by Lonnberg[37] and Butorina[38]. Details of the Rietveld refinement of all the samples can be found in the Support Information. The small discrepancy of the cell parameters was likely attributed to the sample displacement factor as all samples were in wire-form to be measured. The average size of the WC and W_2C crystallite was determined to be 49 nm and 43 nm, respectively.

For the deposition time of 1 hour (Figure 1 a), both WC and W_2C phases were present at 2000 to 2300 ºC. The amount of WC in the outer-shell is greater than that of W_2C. This is in agreement with the W-C phase diagram[22,39,40] which indicates that WC is more favorable than W_2C when there is sufficient C present. When the temperature was increased to 2400 ºC, however, only peaks from W_2C were observed with the most intense one appearing at 2θ = 70.0º. It is also noted that at this high temperature of 2400 ºC, the peaks from W disappeared. Same is observed with the alloyed filaments prepared at 2 hours (Figure 1b). One note is that the amount of WC is significantly reduced at 2100 - 2300 ºC after 2 hours as compared to those after 1 hour. Therefore, the exposure of the heated filaments to TMDSCB carburized the W metal to form crystallined WC and W_2C at 2000 - 2300 ºC. With increasing temperature and deposition time, the carbon-rich WC phase was converted to form W_2C. When the temperature was increased to 2400 ºC, a pure W_2C layer was formed.

The cross-sectional SEM image of the alloyed filament prepared after 1-hour exposure to TMDSCB at 2000 ºC is shown in Figure 2a. According to our previous study[10] using Auger electron spectroscopy (AES), the outside layer under this condition is from the W_2C phase which was converted mainly from the surface WC. Figure 2 b-f showed the cross-sectional images of the filaments prepared after 2-hour exposure to TMDSCB at different temperatures in the range of 2000 - 2400 ºC. The thickness of the outside W_2C layer increases with the temperatures. This is also observed for the filaments prepared after the shorter deposition time of 1 hour at this temperature. The average growth rate at 2000 and 2100 ºC was determined to be 0.74 $\mu m \cdot min^{-1}$, and it increases to 4.4 $\mu m \cdot min^{-1}$ at the higher temperatures of 2300 and 2400 ºC. Zeiler *et al.*[8] reported a W_2C growth rate of 4 $\mu m \cdot min^{-1}$ when using the mixture of 1% CH_4 and 99% H_2 to carburize the metal filament at 2450 ºC. Our results show that similar or slightly higher growth rate can be obtained at lower temperature when using TMDSCB as the source gas to replace the CH_4/H_2 mixture.

At the two low-end temperatures of 2000 and 2100 ºC examined in this work when the W_2C layer boundary is visible, it is found that the layer thickness generally increase with deposition time as shown in Figure 3. The growth of W_2C for the first 3 hours at 2000 ºC follow a parabolic law where the thickness is linearly proportional to the square root of time. This suggests that the growth is controlled by a diffusion process. The corresponding diffusion coefficient is determined to be 4.1×10^{-13} $m^2 \cdot s^{-1}$, which is close to the carbon diffusion coefficients in tungsten subcarbide - W_2C reported in the literature.[41]

The XRD patterns for the alloyed filaments prepared at longer time of 3 and 4 hours, respectively, were shown in Figure 4a and 4b. For a deposition time of 3 hours, the amount of WC phase increases with increasing temperature. This is different from the observations for the

filaments prepared at 1 and 2 hours. At the highest temperature of 2400 ºC for the deposition time of 3 hours, aside from the W_2C phases observed at 1 - 2 hours, the WC re-appears. The peaks from W metals were no longer there, similar to those observed for the shorter deposition time. At an even longer deposition time of 4 hours, the peaks from the W_2C phase disappeared at 2400 ºC. The outer layer of the filament was now composed of mainly WC, with the most intense peak observed at $2\theta = 48.5^{\circ}$. It should be noted that both W and WC contribute to the peak at 73.3 - 73.5°. To determine the amount of W contribution to this peak intensity, the two other characteristic peaks of W at 40.6, 58.6º and the intensity ratios in pure W need to be taken into account. The phase composition determined from the Rietveld refinement of the as-prepared sample for 2400 ºC at 1 hour showed that 97.54% is from WC with the remaining 2.46% from W. The observed XRD patterns in Figures 1 to 4 suggests that once the W filaments are fully carburized to form the W_2C phase after 1- and 2-hour exposure to TMDSCB at 2400 ºC, further exposure leads to the conversion now from W_2C to the C-rich phase, WC. At 2400 ºC after 4 hour exposure to TMDSCB, a WC layer with no contamination from the W_2C phase has been obtained at the outside surface of the filament. Since no definite boundary can be observed in the cross-section SEM images of the filament, the exact thickness of the WC layer cannot be determined.

The resistances of the carburized filaments were monitored in-situ in our experiments. In each run, the resistance increases continuously with the deposition time, as shown in Figure 5a for the run of 2400 ºC and 1 hour. The resistance increases much faster in the first 10 minutes, followed by a slower increase for the remaining time. The initial quick increase in the resistance is due to the increased power needed for the decomposition of TMDSCB on the filament to produce methyl radicals, whereas carburization contributes to the consistence increase during the

1 hour deposition time. The terminal resistance for each carburized filament represented in Figure 5b clearly shows that raising the temperature results in an increase in resistance. It is known that the resistivity of tungsten carbides is higher than their pure metal component. The electrical resistivity of W_2C and WC at room temperature is reported to be 8.0×10^{-5} $\Omega \cdot cm^{-1}$ and 2.2×10^{-5} $\Omega \cdot cm^{-1}$, respectively, whereas that for the pure W metal is 5.5×10^{-6} $\Omega \cdot cm^{-1}$.[42] The total resistance, R_{total}, of the carburized tungsten filament with a radius r_2 and a residual metal core of radius r_1 can be calculated using a mathematical model (Equation 3) proposed by Okoli et al.[41]

$$R_{total} = L\left(\frac{A_1(\rho_2-\rho_1)}{\rho_2\rho_1} + \frac{A_2}{\rho_2}\right)^{-1} \quad (3)$$

where L is the length of the filament, A_1 is the cross-section area of the remaining metal core, A_2 is the area for the entire wire, ρ_1 and ρ_2 are the electrical resistivity of the metal and carbide, respectively. Assuming a W_2C layer on the outside and W in the core, the calculated resistance for all the filaments prepared is listed in Table 1.

For the shorter deposition time of 1 and 2 hours, the total resistance calculated from Eqn. (3) generally agrees well with the value obtained from our experimental measurements. This supports our conclusion with the XRD analysis that the formation of W_2C phase is dominant at these deposition time. At 2400 ºC, only W_2C phase exists based on the XRD patterns. However, one is not sure if the filaments are fully carburized to form W_2C under these conditions since the penetration depth for XRD analysis is up to 30 μm. Assuming the whole cross section is made of W_2C with no remaining W metal core, the resistances for the two alloyed filaments prepared at 2400 ºC/1 hr, and 2400 ºC /2 hr were calculated to be 0.589, and 0.619 Ω, respectively (Table 1), which in good agreement with the experimental values. If we model the resistance calculations based on a remaining metal core defined by the vague interface shown in the cross-sectional

SEM images (see Figure 2f), the discrepancy between the theoretical and experimental resistance values becomes larger. Therefore, the resistance measurements seem to suggest that the tungsten filament is fully carburized to W_2C under these conditions. It is unclear at this point why there is a vague interface in the cross-sectional SEM image shown in Figure 2f.

At the longer deposition time of 3 - 4 hours, the amount of WC phases increases as shown in the XRD patterns in Figure 4. Therefore, the mismatch between the calculated and experimental resistance values starts to show. For the filament prepared at 2400 ºC after 4 hour deposition time, the difference is as large as -0.291 Ω, representing a decrease of 36%. Since the electrical resistivity of WC at higher temperatures is not known and the boundary between the W_2C and WC phases is not clearly visible, the modeling of the resistance of the filaments consisting mainly of WC and W_2C is currently not possible.

Conclusions

This work demonstrates a new method of forming crystalline tungsten carbides. By heating the tungsten metal filament to high temperatures of 2000 to 2400 ºC in the environment of a gaseous mixture of 1,1,3,3-tetramethyl-1,3-disilacyclobutane (TMDSCB) and He, crystalline W_2C and WC has been prepared in the hot-wire CVD process. XRD combined with in-situ resistance measurements has been used to monitor the growth of WC and W_2C phases on the heated W wires exposed to TMDSCB. A pure W_2C or WC layer can be formed by tuning the deposition parameters. At a deposition time of 1 and 2 hours, exposure to TMDSCB led to the formation of both WC and W_2C on the filament surface at 2000 to 2300 ºC. With increasing temperature and deposition time, the carbon-rich WC phase was converted to form W_2C. At 2400 ºC, a pure W_2C phase was formed. The formation of W_2C is controlled by diffusion of

carbon into the filament interior. The filament resistance measurements suggest that the metal filaments are fully carburized to form W_2C after 1 - 2 hour exposure to TMDSCB at 2400 ºC with a growth rate of 4.4 $\mu m \cdot min^{-1}$. At longer deposition time of 3 - 4 hours, once the metal filament is fully carburized to form W_2C, the carbon-rich WC phase starts to form on the outside layer upon further exposure to TMDSCB. A WC layer with no contamination from the W_2C phase was found to be formed at 2400 ºC and 4-hour deposition time. Our study on the tungsten carbide growth at different temperature and deposition time has also shed light onto the growth mechanism of the two phases, WC and W_2C, aiming towards a better understanding of the process. In addition, with the knowledge of the tungsten carbide phases formed on the filament under different conditions, further work can be performed on the effect of different phases on its catalytic ability.

Acknowledgments

This work was funded by the Natural Sciences and Engineering Council of Canada (NSERC). Access to SEM was kindly provided by the Microscope and Imaging Facility at the University of Calgary.

Support Information Available: The Rietveld refinement of the XRD data for all the samples can be found in the Support Information. This material is available free of charge via the Internet at http://pubs.acs.org.

References

1. Proceedings of the 6th International Conference on Hot-wire CVD (Cat-CVD) Processes, 2011 *Thin Solid Films*, Vol. 519, Issue 14.

2. Holt, J. K.; Swiatek, M.; Goodwin, D. G.; Atwater, H. A., The Aging of Tungsten Filaments and its Effect on Wire Surface Kinetics in Hot-wire Chemical Vapor Deposition, *J. Appl. Phys.* **2002,** *92*, 4803-4808.

3. van Veenendaal, P. A. T. T.; Gijzeman, O. L. J.; Rath, J. K.; Schropp, R. E. I., The Influence of Different Catalyzers in Hot-wire CVD for the Deposition of Polycrystalline Silicon Thin Films, *Thin Solid Films* **2001,** *395*, 194-197.

4. Honda, K.; Ohdaira, K.; Matsumura, H., Study of Silicidation of Tungsten Catalyzer during Silicon Film Deposition in Catalytic Chemical Vapor Deposition, *Jpn. J. Appl. Phys.* **2008,** *47*, 3692-3698.

5. Tong, L.; Sveen, C. E.; Shi, Y. J., Study of Tungsten Filament Aging in Hot-wire Chemical Vapor Deposition with Silacyclobutane as a Source Gas and the H_2 Etching Effect, *J. Appl. Phys.* **2008**, *103*, 123534-1 - 123534-6.

6. Sveen, C. E.; Shi, Y. J., Effect of Filament Temperature and Deposition Time on the Formation of Tungsten Silicide with Silane, *Thin Solid Films* **2011,** *519,* 4447-4450.

7. Rye, R. R., Hot-filament-activated Chemical Vapor Deposition of Carbon: Film Growth and Filament Reactions, *J. Appl. Phys.* **1994,** *76*, 1220-1227.

8. Zeiler, E.; Schwarz, S.; Rosiwal, S. M.; Singer, R. F. Structural Changes of Tungsten Heating Filaments during CVD of Diamond, *Mat. Sci. Eng. A-Struct* **2002,** *335,* 236-245.

9. Comerford, D. W.; D'Haenens-Johansson, U. F. S.; Smith, J. A.; Ashfold, M. N. R.; Mankelevich, Y. A., Filament Seasoning and its Effect on the Chemistry Prevailing in Hot

Filament activated Gas Mixtures Used in Diamond Chemical Vapor Deposition, *Thin Solid Films,* **2008,** *516,* 521-525.

10. Tong, L.; Shi, Y. J., Carburization of Tungsten Filament in a Hot-wire Chemical Vapor Deposition Process Using 1,1,3,3-tetramethyl-1,3-disilacyclobutane, *ACS Appl. Mater. Inter.* **2009,** *1*, 1919-1926.

11. Mahan, A. H., Hot Wire Chemical Vapor Deposition of Si-containing Materials for Solar Cells, *Solar Energ. Mat. Sol. C* **2003,** *78*, 299-327.

12. Moustakas, T. D., The Role of the Tungsten Filament in the Growth of Polycrystalline Diamond Films by Filament-assisted CVD of Hydrocarbons, *Solid State Ionics* **1989,** *32-3*, 861-868.

13. Toth, L. E. *Transition Metal Carbides and Nitrides*; Academic Press: New York, 1971.

14. Chen, J. G., Carbide and Nitride Overlayers on Early Transition Metal Surfaces: Preparation, Characterization, and Reactivities, *Chem. Rev.* **1996,** *96*, 1477-1498.

15. Levy, R. B.; Boudart, M., Platinum-like Behavior of Tungsten Carbide in Surface Catalysis, *Science* **1973,** *181*, 547-549.

16. Joo, J. B.; Kim, J. S.; Kim, P.; Yi, J., Simple Preparation of Tungsten Carbide Supported on Carbon for Use as a Catalyst Support in a methanol electro-oxidation, *Mater. Lett.* **2008,** *62*, 3497-3499.

17. Esposito, D. V.; Chen, J. G., Monolayer Platinum Supported on Tungsten Carbides as Low-cost electrocatalysts: Opportunities and Limitations, *Energ. Environ. Sci.* **2011,** *4*, 3900-3912.

18. Kojima, I.; Miyazaki, E.; Inoue, Y.; Yasumori, I., Catalytic Activities of TiC, WC, And TaC for Hydrogenation of Ethylene, *J. Catal.* **1979,** 59**,** 472-474.

19. Hwu, H. H.; Chen, J. G., Surface Chemistry of Transition Metal Carbides, *Chem. Rev.* **2005,** *105*, 185-212.

20. Jiang, X. L.; Gitzhofer, F.; Boulos, M. I.; Tiwari, R., Reactive Deposition of Tungsten and Titanium Carbides by Induction Plasma, *J. Mater. Sci.* **1995,** *30*, 2325-2329.

21. Chitica, N.; Gyorgy, E.; Lita, A.; Marin, G.; Mihailescu, I. N.; Pantelica, D.; Petrascu, M.; Hatziapostolou, A.; Grivas, C.; Broll, N.; Cornet, A.; Mirica, C.; Andrei, A., Synthesis of Tungsten Carbide Thin Films by Reactive Pulsed Laser Deposition, *Thin Solid Films* **1997,** *301*, 71-76.

22. Palmquist, J. P.; Czigany, Z.; Oden, M.; Neidhart, J.; Hultman, L.; Jansson, U., Magnetron Sputtered W-C Films with C_{60} as Carbon Source, *Thin Solid Films* **2003,** *444***,** 29-37.

23. Zellner, M. B.; Chen, J. G., Surface Science and Electrochemical Studies of WC and W_2C PVD Films as Potential Electrocatalysts, *Catal. Today* **2005,** *99*, 299-307.

24. Zheng, H. J.; Ma, C. N.; Wang, W.; Huang, J. G., Nanorod Tungsten Carbide Thin Film and its Electrocatalytic Activity for Nitromethane Electroreduction, *Electrochem. Commun.* **2006,** *8,* 977-981.

25. Beadle, K. A.; Gupta, R.; Mathew, A.; Chen, J. G.; Willis, B. G. Chemical Vapor Deposition of Phase-rich WC Thin Films on Silicon and Carbon Substrates, *Thin Solid Films* **2008,** *516,* 3847-3854.

26.Weigert, E. C.; Esposito, D. V.; Chen, J. G., Cyclic Voltammetry and X-ray Photoelectron Spectroscopy Studies of Electrochemical Stability of Clean and Pt-modified Tungsten and Molybdenum Carbide (WC and Mo_2C) Electrocatalysts, *J. Power Sources*, **2009**, *193*, 501-506.

27. Scottlemeyer, A. L.; Weigert, E. C.; Chen, J. G., Tungsten Carbides as Alternative Electrocatalysts: From Surface Science Studies to Fuel Cell Evaluation, *Ind. Eng. Chem. Res.* **2011**, *50*, 16-22.

28. Gusel'nikov, L. E.; Avakyan, V. G.; Guselnikov, S. L., Effect of Geminal Substitution at Silicon on 1-Sila- and 1,3-Dislacyclobutanes' Strain Energies, Their 2+2 Cycloreversion Enthalpies, and Si=C π-bond Energies in Silenes, *J. Am. Chem. Soc.* **2002,** *124*, 662-671.

29. Tong, L.; Shi, Y. J., A Mechanistic Study of Gas-phase Reactions with 1,13,3-tetranethyl-1,3-dislacyclobutane in the Hot-wire Chemical Vapor Deposition Process, *Thin Solid Films* **2009,** *517*, 3461-3465.

30. Shi, Y. J.; Tong, L.; Eustergerling, B. D.; Li, X. M., Silicidation and Carburization of the Tungsten Filament in HWCVD with Silacyclobutane Precursor Gases, *Thin Solid Films* **2011,** *519*, 4442-4446.

31. Shi, Y. J.; Lo, B.; Tong, L.; Li, X. M.; Eustergerling, B. D.; Sorensen, T. S., In-situ Diagnostics of the Decomposition of Silacyclobutane on a Hot Filament by Vacuum Ultraviolet Laser Ionization Mass Spectrometry, *J. Mass Spectrom.* **2007,** *42***,** 575-583.

32. Li, X. M.; Eustergerling, B. D.; Shi, Y. J., Mass Spectrometric Study of Gas-phase Chemistry in a Hot-wire Chemical Vapor Deposition Reactor with Tetramethylsilane, *Int. J. Mass Spectrom.* **2007,** *263,* 233-242.

33. Eustergerling, B. D.; Heden, M.; Shi, Y. J., Development of a New Laser Induced Electron Impact Ionization Source for Studying the Hot-wire Chemical Vapor Deposition Chemistry of Silane-ammonia Mixtures, *J. Anal. Atom Spectrom.* **2008,** *23*, 1590-1598.

34. Shi, Y. J.; Eustergerling, B. D.; Li, X. M., Mass Spectrometric Study of Gas-phase Chemistry in the Hot-wire Chemical Vapor Deposition Processes of SiH_4/NH_3 Mixtures, *Thin Solid Films* **2008,** *516*, 506-510.

35. Toby, B. H., EXPGUI, a Graphic User Interface for GSAS, *J. Appl. Crystallogr.* **2001**, *34*, 210-213.

36. Davey, W. P., Precision Measurements of the Lattice Constants of Twelve Common Metals, *Phys. Rev.* **1925,** *25*, 753-761.

37. Lonnberg, B.; Lundstrom, T.; Tellgren, R., A Neutron Powder Diffraction Study of Ta_2C and W_2C, *J. Less-Common Met.* **1986,** *120,* 239-245.

38. Butorina, L. N., *Sov. Phys. Crystallography (Engl. Transl.)* **1990,** *5*, 216-222.

39. Kurlov, A. S.; Gusev, A. I., Tungsten Carbides and W-C Phase Diagram, *Inorg. Mater.* **2006**, *42*, 121-127.

40. Sara, R. V., Phase Equilibria in the System Tungsten-Carbon, *J. Am. Ceram. Soc.* **1965**, *48*, 251-257.

41. Okoli, S.; Haubner, R.; Lux, B., Carburization of Tungsten and Tantulum Filaments during Low-pressure Daimond Deposition, *Surf .Coat. Tech.* **1991,** *47*, 585-599.

42. *CRC Handbook of Chemistry and Physics*; 56^{th} Edition, West R C, Ed.; CRC Press: Cleveland, Ohio, 1975 - 1976.

Table 1 The total resistance of filament measured from the experiments and from theoretical calculations

Temperature (ºC)	Time (hour)	ρ of W[a] (Ω cm)	ρ of W_2C[b] (Ω cm)	Calculated R (Ω)	Experimental R (Ω)
2000	1	6.69×10^{-5}	1.21×10^{-4}	0.398	0.423
2000	2			0.456	0.46
2000	3			0.457	0.499
2000	4			0.456	0.478
2100	1	7.04×10^{-5}	1.24×10^{-4}	0.471	0.41
2100	2			0.461	0.462
2100	3			0.489	0.416
2100	4			0.531	0.476
2200	1	7.39×10^{-5}	1.25×10^{-4}	0.490	0.5
2200	2			0.509	0.511
2200	3			0.512	0.524
2200	4			0.500	0.556
2300	1	7.75×10^{-5}	1.28×10^{-4}	0.570	0.556
2300	2			0.549	0.583
2300	3			0.435	0.602
2300	4			0.589	0.615
2400	1	8.10×10^{-5}	1.30×10^{-4}	0.589	0.582
2400	2			0.619	0.677
2400	3			0.564	0.701
2400	4			0.514	0.805

[a] The values for the electrical resistivity (ρ) of W at different high temperatures are obtained from Ref. 38; [b] The ρ value of W_2C at 2200 ºC is from Ref. 37. The ρ values of W_2C at other temperatures are calculated from the $\Delta\rho/\Delta T$ determined from the data at 2200 ºC and room temperature, assuming a linear dependence of ρ on T;

Figure Captions

Figure 1. XRD patterns of alloyed filaments prepared at various temperatures in the range of 2000 to 2400 ºC for a deposition time of (a) 1 hour, and (b) 2 hours. The XRD pattern of a new W filament is presented in (a) for comparison. Indexing labels: WC (Blue), and W_2C (Red).

Figure 2. Cross-sectional SEM images of alloyed filaments prepared (a) at 2000 ºC for 1 hour, and for 2 hours at (b) 2000 ºC, (c) 2100 ºC, (d) 2200 ºC, (e) 2300 ºC, and (f) 2400 ºC.

Figure 3. The W_2C layer thickness as a function of the square root of deposition time for filaments prepared at 2000 ºC indicating a parabolic dependence.

Figure 4. XRD patterns of alloyed filaments prepared at various temperatures in the range of 2000 to 2400 ºC for a deposition time of (a) 3 hours, and (b) 4 hours. The XRD pattern of a new W filament is presented in (a) for comparison. Indexing labels: WC (Blue), and W_2C (Red).

Figure 5. (a) The resistance as a function of time for the filament prepared at 2400 ºC and a deposition time of 1 hour, and (b) the terminal resistance for all 20 alloyed filaments prepared at different temperatures and time.

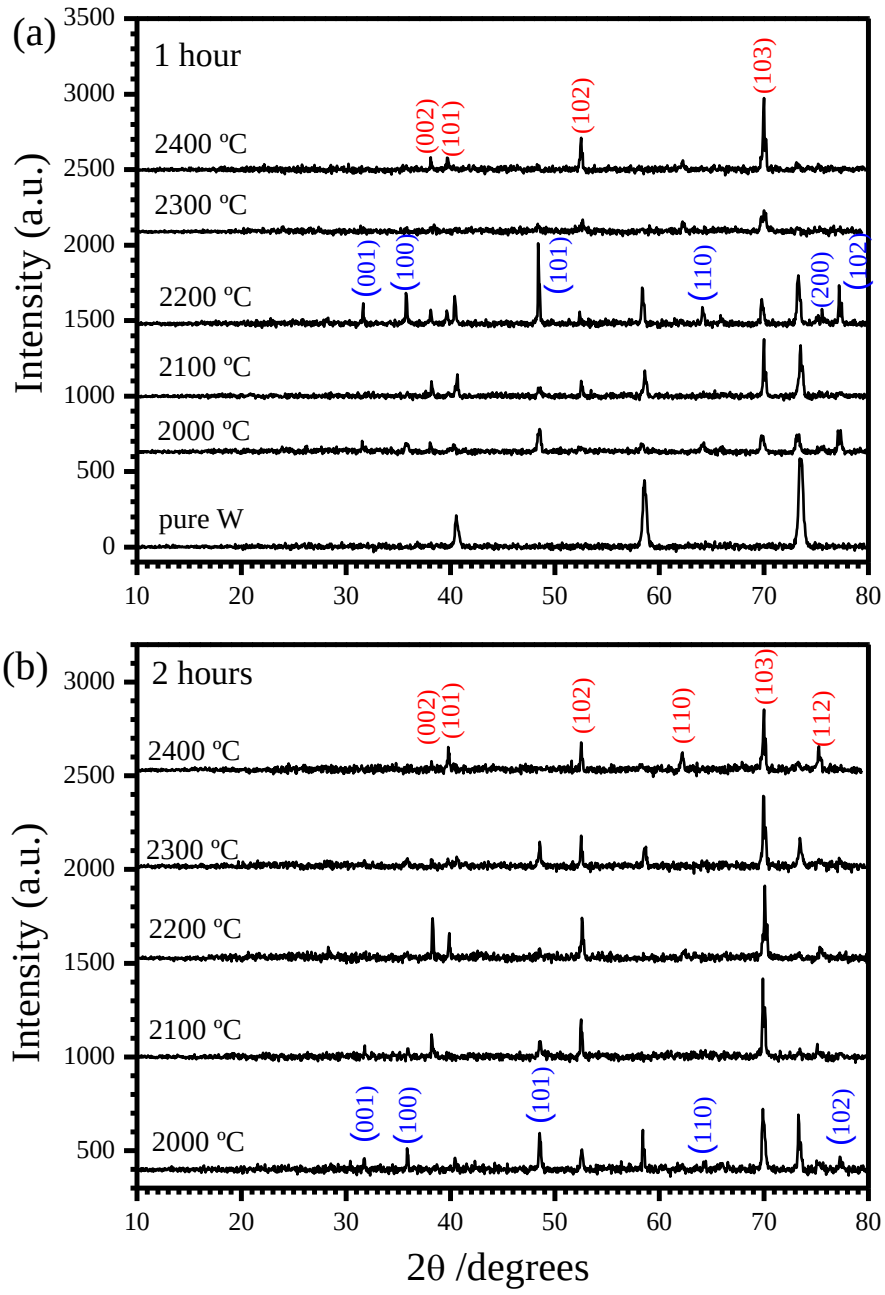

Figure 1. XRD patterns of alloyed filaments prepared at various temperatures in the range of 2000 to 2400 ºC for a deposition time of (a) 1 hour, and (b) 2 hours. The XRD pattern of a new W filament is presented in (a) for comparison. Indexing labels: WC (Blue), and W_2C (Red)

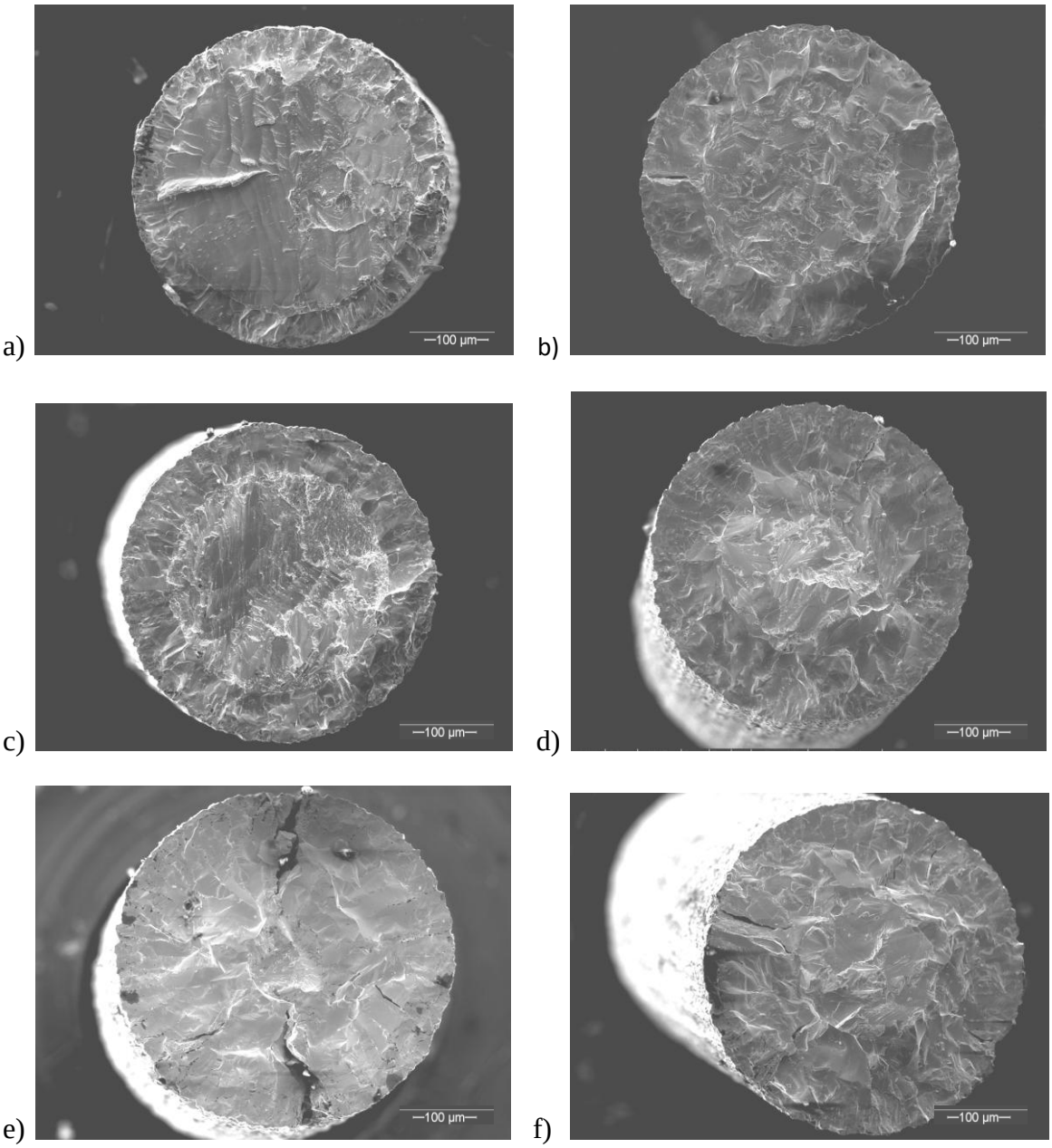

Figure 2. Cross-sectional SEM images of alloyed filaments prepared (a) at 2000 ºC for 1 hour, and for 2 hours at (b) 2000 ºC, (c) 2100 ºC, (d) 2200 ºC, (e) 2300 ºC, and (f) 2400 ºC

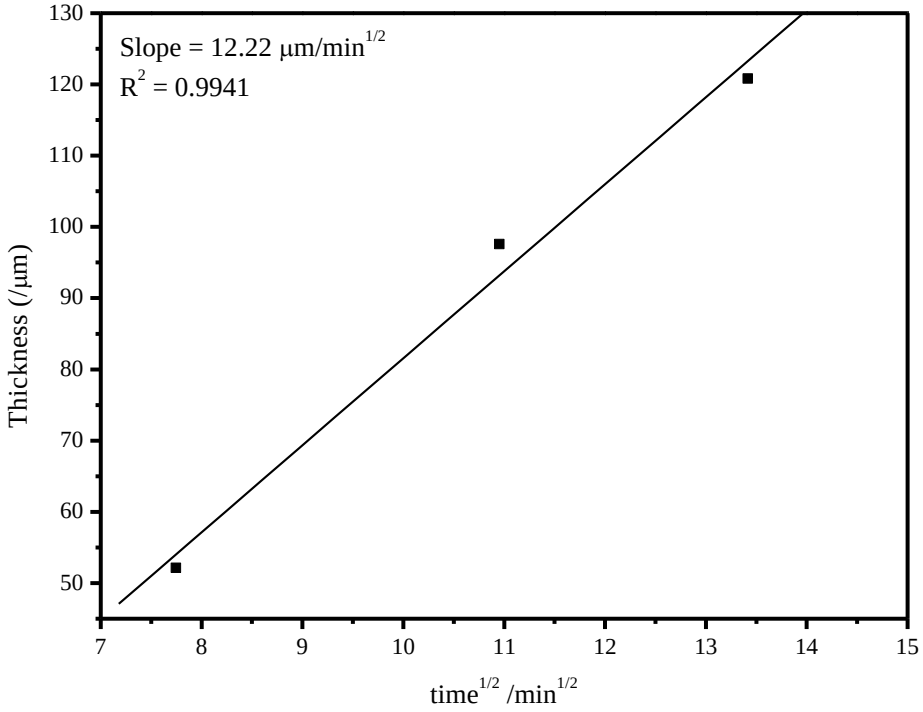

Figure 3. The W_2C layer thickness as a function of the square root of deposition time for filaments prepared at 2000 ºC indicating a parabolic dependence

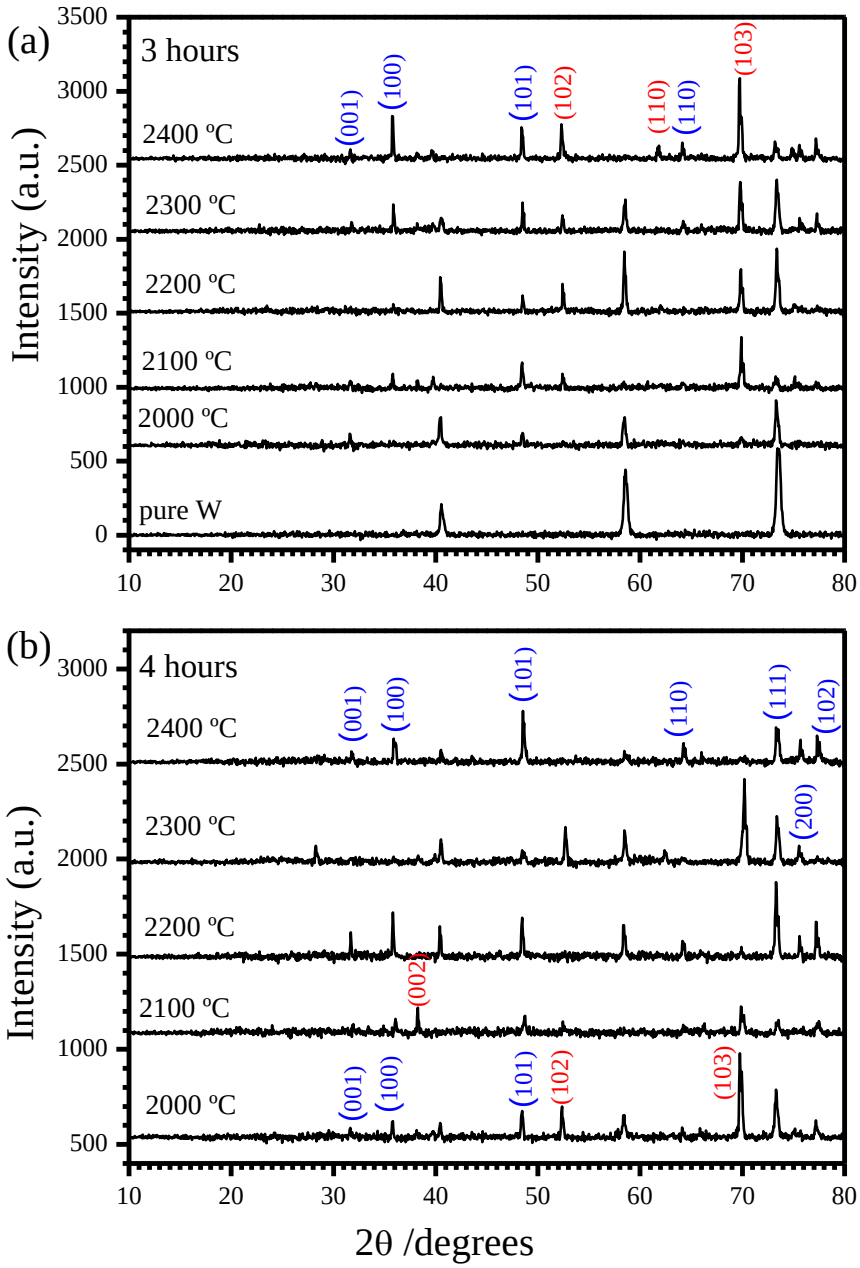

Figure 4. XRD patterns of alloyed filaments prepared at various temperatures in the range of 2000 to 2400 ºC for a deposition time of (a) 3 hours, and (b) 4 hours. The XRD pattern of a new W filament is presented in (a) for comparison. Indexing labels: WC (Blue), and W_2C (Red)

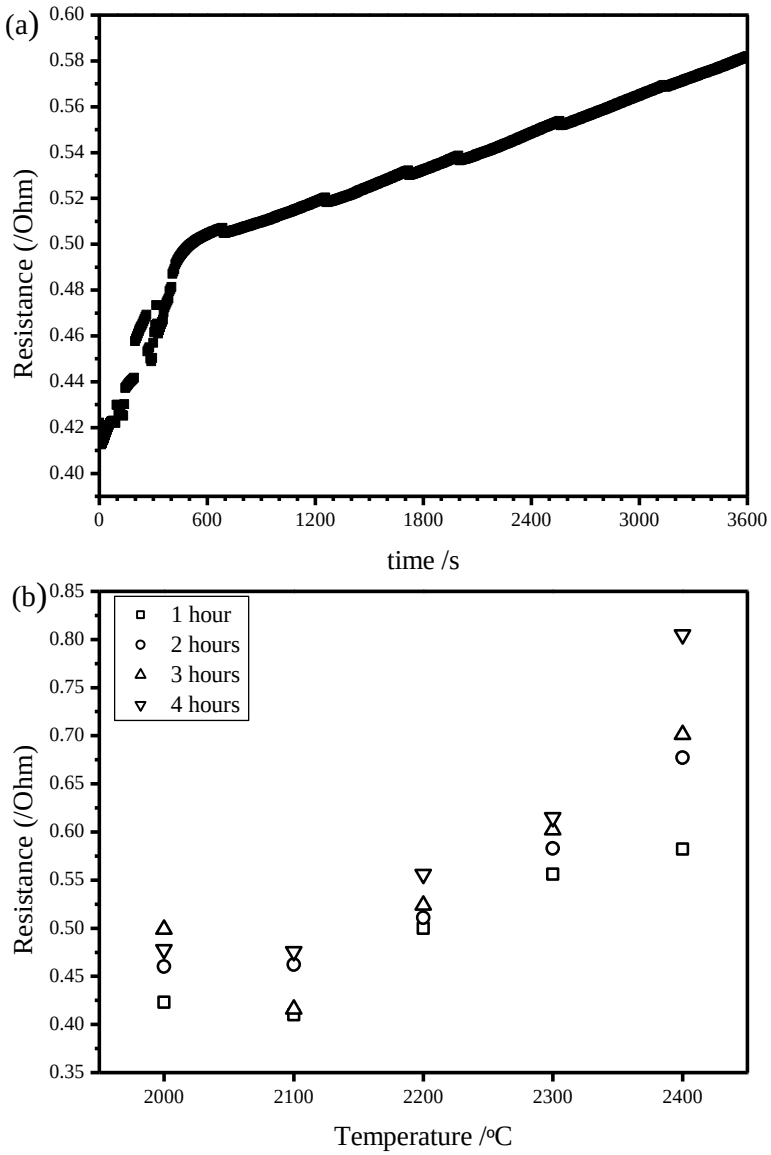

Figure 5. (a) The resistance as a function of time for the filament prepared at 2400 °C and a deposition time of 1 hour, and (b) the terminal resistance for all 20 alloyed filaments prepared at different temperatures and time

Table of Content